

Stability of the vertical bearing structures of the Syracuse Cathedral: experimental and numerical evaluation

Alberto Carpinteri · G. Lacidogna · S. Invernizzi ·
A. Manuello · L. Binda

Received: 10 May 2008 / Accepted: 17 September 2008 / Published online: 27 September 2008
© RILEM 2008

Abstract In the present paper the results from a recent monitoring campaign and numerical analysis performed on the ancient Cathedral of Syracuse in Sicily are presented. The acoustic emission (AE) technique is adopted to assess the damage pattern evolution. The localization of the propagating cracks is obtained using six synchronized AE sensors. A clear correlation between the regional seismic activity and the AE acquisition data is shown. In fact the AE count rate presents peaks corresponding to the main seismic events. In addition, a numerical analysis of the vertical bearing structures of the Cathedral is presented. The nonlinear Finite Element model is particularly refined to account for the cracking in the most damaged pillar. Some recent seismic events in the area acted as crack propagators. The crack occurrence obtained from the numerical analysis agrees quite well with the crack localization provided by the AE monitoring.

Keywords Acoustic emission technique · Damage localization · Damage evolution · Seismic events · Numerical modelling of cracking

1 Introduction

The Cathedral of Syracuse (Sicily—Italy) is located in the higher zone of the Ortigia island. This region of Sicily has been belonging to the UNESCO World Heritage List since 2005. The Cathedral of Syracuse is the result of the transformation of the ancient Athena's Greek Temple (5th century B.C.), with modifications that have also been consequence of the damages caused by earthquakes. The ancient temple had 14 lateral columns and six in the front. The Cathedral incorporated many of them, as it is nowadays still visible, while other columns of the present structure were built with the salvage remains from the temple cell. At the present time, the structure shows an extended damage pattern, especially in four of the nave pillars [1].

In recent years, the authors have been working on the development of a method for the assessment of materials and structures based on the spontaneous release of pressure waves originated by the evolution of damage. This monitoring technique, referred to as acoustic emission (AE), is non invasive and non destructive and therefore is ideally suited for the control of historic and monumental structures in

A. Carpinteri (✉) · G. Lacidogna · S. Invernizzi ·
A. Manuello
Department of Structural Engineering and Geotechnics,
Politecnico di Torino, Corso Duca degli Abruzzi, 24,
Torino, Italy
e-mail: alberto.carpinteri@polito.it

L. Binda
Department of Structural Engineering,
Politecnico di Milano, Milan, Italy

seismic areas [2–4]. With this technique, if it is not known, the initial position of the damage can be determined with the aid of a multiplicity of sensors and through triangulation [5–7]. Once the damaged portion of a structure has been located, it becomes possible to evaluate the stability of the evolving damage, which may either gradually stop or propagate at an ever faster rate. In this study, the AE technique was used to determine the damage level in a pillar that was part of the vertical bearing structure of the Cathedral of Syracuse (Sicily). Beside the experimental research, a numerical simulation based on the Finite Element Method is performed, which is able to catch the main non linear features of the mechanical behaviour such as fracture nucleation, fracture propagation and time dependency. The most damaged pillar has been modelled in details, providing an accurate description of the blocks interaction by means of discrete interface elements. The main goal is to link the dissipated energy, acquired from the AE, and the fracture localization with the results obtained numerically [8, 9]. The numerical model shows the cracks develop due to the seismic load,

according also to the experimental evidence by the AE acquisition.

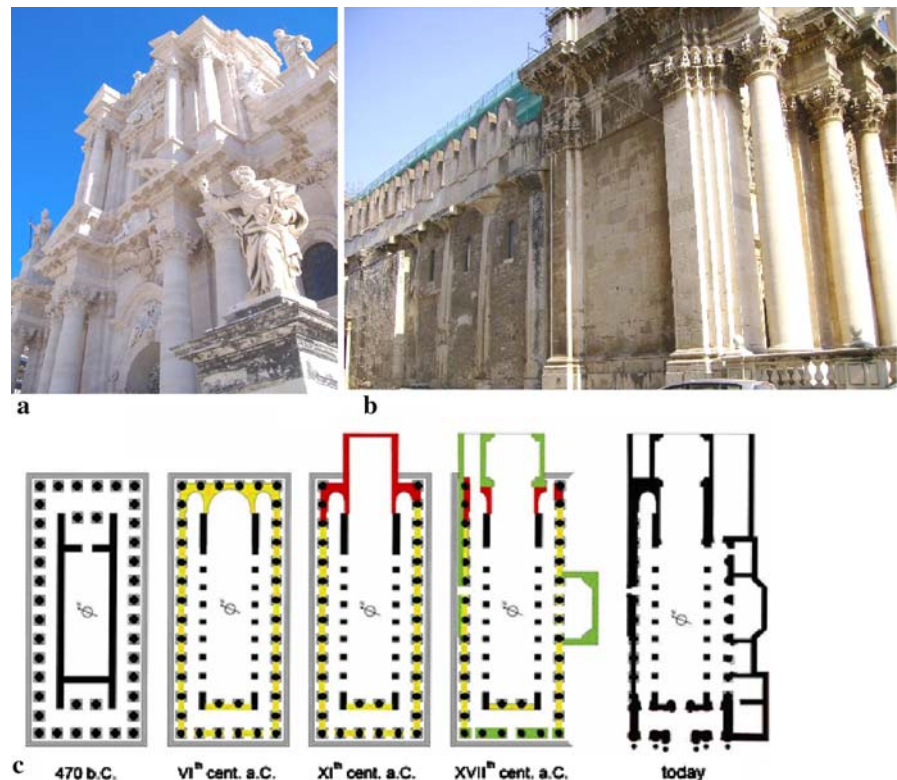
2 Syracuse Cathedral and state of preservation

In the 6th century AD, the 5th century B.C. Greek temple of Athena in Syracuse, was transformed into a Catholic Church, and successively became the Cathedral of the City; the building was frequently modified along the centuries until the present configuration [10–14].

Several styles and structural details belonging to the different times can be recognised: (i) in the external walls the ancient Greek columns and the filling wall between them of the Byzantine time, (ii) the baroque façade, (iii) the added apse and chapels. Furthermore, being Syracuse in a seismic area, the Cathedral was damaged, repaired or partially rebuilt several times [10, 11]. Figure 1a–c shows the Cathedral and the evolution of its plan along the centuries.

The Cathedral pillars have a peculiar interest; they had been obtained cutting out the stonework walls of

Fig. 1 The Syracuse Cathedral and its evolution. The Syracuse Cathedral (a): lateral view (b) and its evolution (c)



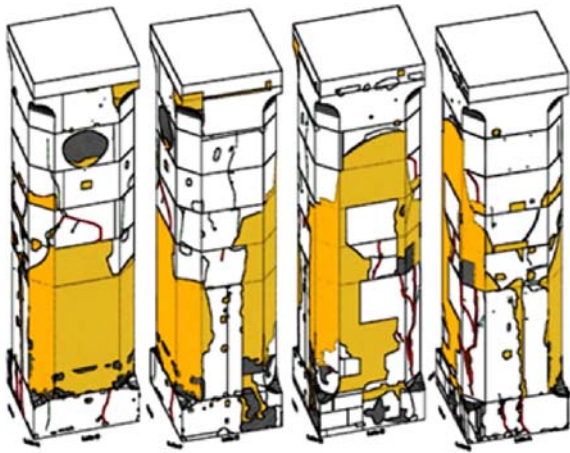
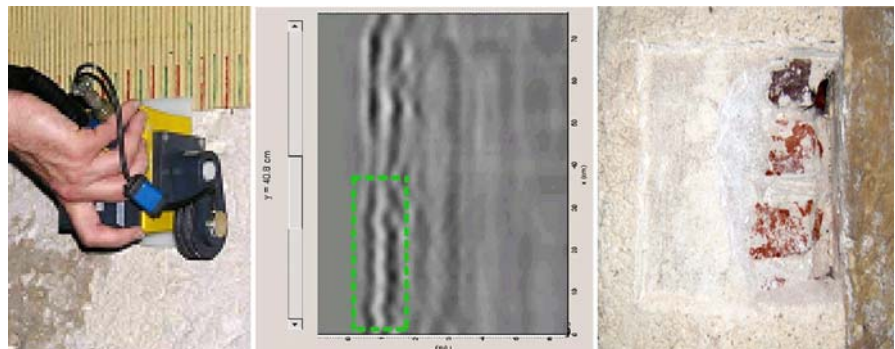


Fig. 2 Cracks pattern survey of the monitored pillar

the internal cell of the Greek temple. The pillars show several repaired areas, replacements, but also several cracks.

In order to evaluate their state of preservation, the extension and the depth of the replacements and the presence of internal defects, an investigation program was planned by the Syracuse Superintendence for Cultural Heritage and the Politecnico di Milano. As a first step, a survey of the pillars with an accurate mapping of the superficial materials, of the defects, of the cracks and of the morphology was carried out. The crack pattern was classified and accurately documented and reported on the geometrical survey. Figure 2 gives an example of this documentation referred to a damaged pillar. The cracks display frequently a vertical pattern due to compressive stresses, whose action is often combined with the compressive-bending stresses caused by frequent earthquakes. In some cases, the corners and part of the stone blocks were spalled off. The mortar traces in these cases denote trials to repair the local

Fig. 3 The radargram shows the presence of regularly spaced diffractions (about every 5–6 cm) at a depth of about 3–4 cm. The inspection proved that these pillars were sometimes repaired with bricks masonry instead of stone



damages. In the survey, repaired cracks were cleared in order to evaluate the evolution of damage.

On the base of this detailed survey, NDT tests were performed in order to investigate the depth of the damage: (i) sonic and ultrasonic to find voids inside the pillars and the depth of the cracks respectively (in some cases up to 400 mm), (ii) thermovision to detect the detachment of renders and repaired parts, (iii) radar to find internal cracks and inclusions (Fig. 3).

The complementarity of these NDTs, already studied in [15, 16], could be successfully exploited to diagnose the state of damage of the pillars [17]. Furthermore, a 2 years monitoring of the cracks development showed an evident trend of size increasing in some of the pillars positioned at the end of the central nave, which suggested a further check of the damage by AE.

3 AE monitoring

3.1 The monitored pillar

The AE monitoring process was performed on a pillar of the Cathedral of Syracuse. The temple had 14 columns along the sides and 6 at front, and some of them, belonging to the peristyle and the stylobate, can still be identified. In the layout of the Cathedral shown in Fig. 4, all the pillars and the columns inside the building are marked with a progressive number.

Basically, the Doric columns are marked with numbers in three ranges: 1–8; 22, 23; 33–40; whereas the pillars, obtained from the calcareous stone masonry of the temple cell, are identified with the remaining numbers. As said above, from the survey of the cracks, it was determined that the pillars in the

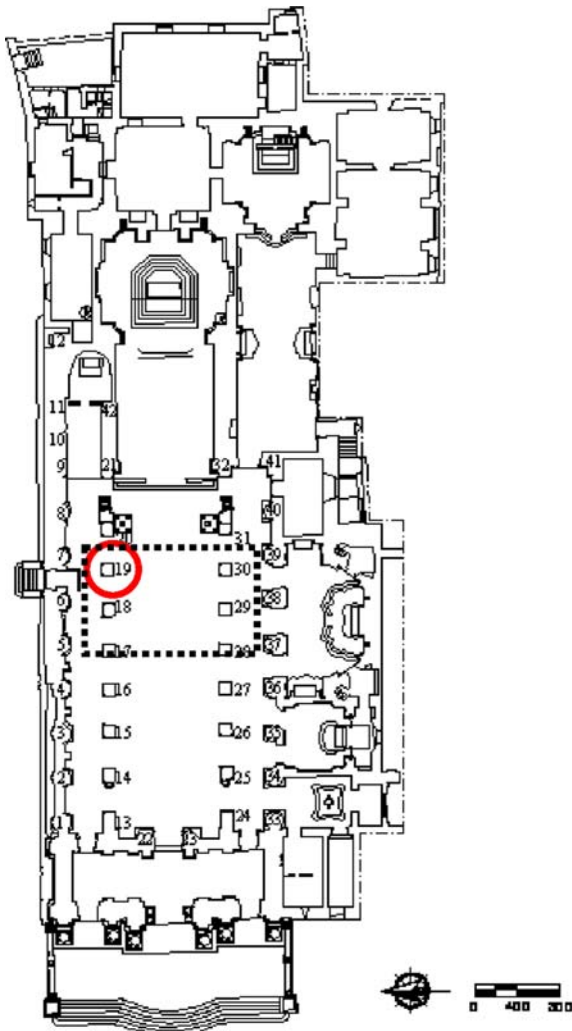


Fig. 4 Plan of the Syracuse Cathedral. Pillars 19, 20, 30 and 31 are pointed out (a). Pillar 19 is indicated by a circle (b)

most critical conditions were nos. 18, 19, 29 and 30, all of them located near the end of the central nave (Fig. 4). These pillars show an appreciable degree of deterioration, due to the presence of added layers of plaster and extended cracking, which in some cases seem to cut through the constituent stone blocks. Pillar no. 19, selected for the application of the AE monitoring technique, is shown in Fig. 4 indicated by a circle.

The pillar no. 19 is likely to be the most damaged. This pillar together with no 18, faces the main altar. It is important to stress the effects of the 1542 earthquake, which produced a great deformation of the perimeter wall close to the pillars nos. 18 and 19.

This could justify the bad state of preservation of these two pillars, characterized by the presence of detached covers and deep cracks on all the prospects. Despite several retrofitting interventions, the section is nowadays reduced. The cracks in these pillars also show larger movements than elsewhere [1].

The pillar (save only thanks to few strengthening works performed in 1926) was thought to be made of limestone blocks, probably installed during the initial construction of the temple dedicated to Athena in the 5th century B.C. The investigation revealed instead the presence of parts made with brick masonry ascribed to the interventions at the beginning of the 20th century (Fig. 5). The lower stiffness of these added masonry parts is probably the cause of the further damage development in the stone.

3.2 AE equipment and “in situ” application details

Monitoring a structure by means of the AE technique allows to detect the occurrence and evolution of stress-induced cracks. Cracking, in fact, is accompanied by the emission of elastic waves which propagate within the bulk of the material. These waves can be received and recorded by piezoelectric (PZT) transducers applied to the surface of the structural elements. The signal is therefore analysed by a measuring system counting the emissions that exceed a certain voltage threshold measured in volts (V). The leading-edge equipment adopted by the authors for the analysis on the vertical bearing structures of the Syracuse Cathedral consists of six units USAM[®], that can be synchronized for multi-channel data processing. The most relevant parameters acquired from the signals (frequencies in a range between 50 and 800 kHz, arrival time, amplitude, duration, number of events and oscillations) are stored in the USAM memory and then downloaded to a PC for a multi-channel data processing (see Fig. 6). Microcracks localisation is performed from this elaboration and the condition of the monitored specimen can be determined [5–7].

The AE sensors have been applied on the middle part of the pillar 19 as shown in Fig. 7a, b. In the Fig. 7a the zones with capillar vertical cracks are indicated by circles. The AE sensors arrangement is represented in Fig. 7a according to the scheme reported in Fig. 7b. The positions of applied sensors

Fig. 5 View of the four sides of the monitored pillar. In the figure the various materials making the pillar are reported

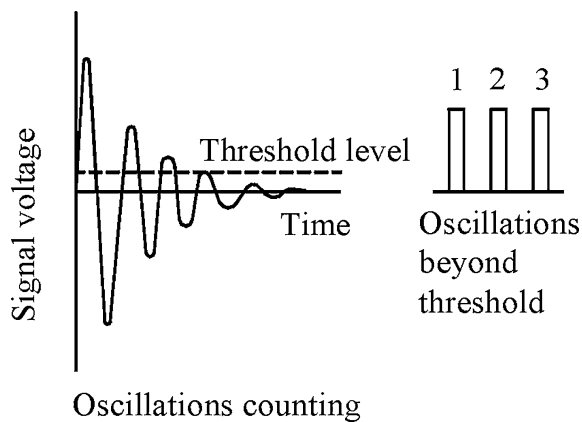
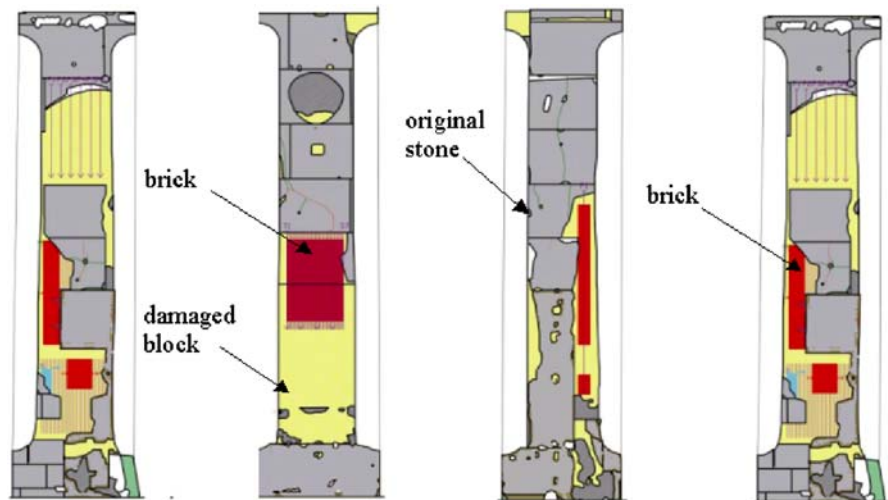


Fig. 6 AE signal identified by the transducer

are listed in Table 1, and the reference frame for the sensors position coordinates is shown in Fig. 7b.

4 Result of the monitoring procedure

The monitoring procedure began at 11:00 a.m. of 19 September 2006 and ended at 12:20 p.m. of 21 January 2007. The data collected were analysed in order to interpret the evolution of damage and determine the positions of AE sources within the pillar. The AE signal received by the transducers is processed by an analyser which counts the oscillations exceeding a certain voltage threshold. This makes it possible to plot the cumulative curves of the count number as measured continuously throughout the monitoring period. This method, referred to as

Ring-Down Counting, is widely used for defect detection purposes (see Fig. 6). As a first approximation, in fact, the count number N , i.e., oscillations per unit time (differential function) can be compared with the quantity of energy released during the monitoring process, and the relative sums (cumulative function) may be assumed to increase proportionately with the widening of the damaged zone. Needless to say, this assumption applies only if the damage evolves slowly [2, 18–20].

From the chart in Fig. 8 it can be seen that the pillar is actually undergoing a deterioration process. In fact if we examine the chart illustrating the differential function of AE counts, we can see a sudden increases in the oscillation peaks occurring at certain intervals over time. It should be also noted that, during the monitoring period, strong seismic actions were recorded in the area, within a radius of ca 50 km around the city of Syracuse. Earthquake data for the period were obtained from website: www.ct.ingv.it/Sismologia/GridSism.asp published by the Seismic Data Analysis Group of Catania (Gruppo di Analisi Dati Sismici—INGV-CT). From the whole record of available data, we selected the seismic events with a local magnitude (MI) greater than 1.2 that occurred during the monitoring period. These events are illustrated in Fig. 8, where the relative occurrence date and magnitude are also given.

The chart in Fig. 8, showing AE monitoring and regional earthquake data, reveals an interesting correlation between the AE activities determined experimentally and seismic events: the timing of the

Fig. 7 View (a) and axonometric projection (b) of the of AE sensor applied to the pillar 19

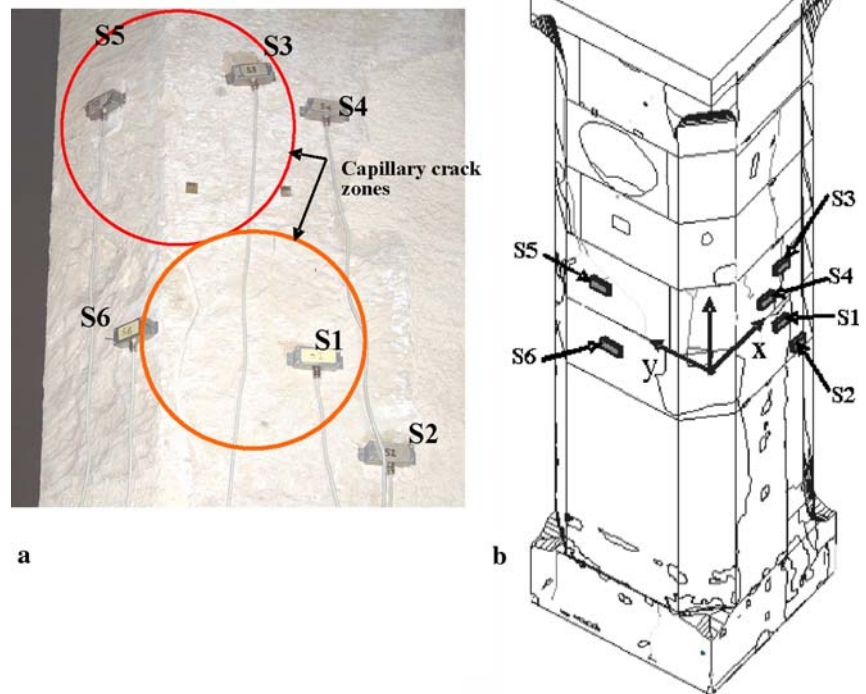


Table 1 Arrangement of the sensors applied to the pillar 19

AE sensors	x (mm)	y (mm)	z (mm)
S1	539.7	0.00	−285
S1	679.7	0.00	−455
S3	434.7	0.00	335
S4	394.7	0.00	265
S5	0.00	410	330
S6	0.00	300	−220

energy peaks measured by means of the AE differential counts is seen to coincide almost invariably with seismic shocks.

This correspondence seems to show how the pillar monitored behaves in a pseudo-stable manner when subject to the vertical loads alone, but has a poor bearing capacity to horizontal or oscillatory actions. A behaviour of this kind was observed by the authors during an earlier monitoring process carried out with the AE technique in site which was also subject to seismic activity [3, 4]. Thus, it may be stated that,

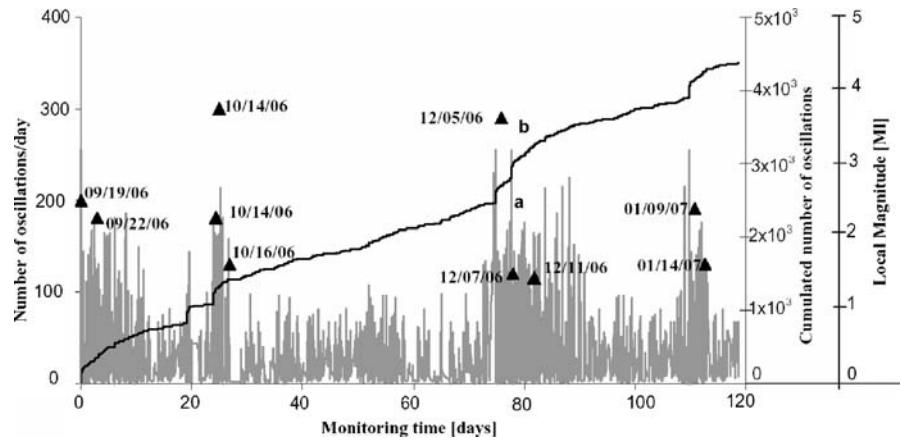
whilst the AE technique finds its primary application in non destructive tests, it is also useful to explore its potential as a monitoring tool in structures exposed to particular environmental conditions, such as seismic activities. As already pointed out by the authors [8], in fact, the two phenomena—AEs on a structural scale and seismic activities on a territorial scale—appear really similar and mutually correlable.

5 Detection of damage in the monitored pillar

5.1 Localisation of acoustic emission sources

The first stage in the localisation method consists in recognising the data needed to identify the AE sources. The equations used for source location in concrete are based on the assumptions of homogeneous and isotropic medium and point-like sources, implying spherical wave propagation. Generally speaking, for single point-like sources in geometries having continuous straight line paths between the

Fig. 8 Differential (a) and cumulated (b) number of AE oscillations during the monitoring time on pillar no. 19. The most relevant seismic events, with the local magnitude value, occurred during the same period are indicated in the graph



source and each receiver, the location technique is called “triangulation procedure”. During the first stage, the groups of signals, recorded by the various sensors, that fall into time intervals compatible with the formation of microcracks in the volume analysed, are identified. These time intervals, of the order of micro-seconds, are defined on the basis of the presumed speed of transmission of the waves (P) and the mutual distance of the sensors applied to the surface of the material.

It is usual to assume that the amplitude threshold of $100 \mu\text{V}$ of the non-amplified signal is appropriate to distinguish between P-wave and S-wave arrival times. In fact, P-waves are usually characterized by signals of higher value [7].

In the second stage, when the formation of microcracks in a three-dimensional space is analysed, the triangulation technique can be applied if signals recorded by at least five sensors fall into the time intervals. Thus, with this procedure it is possible to define both the position of the microcracks in the volume and the speed of transmission of P-waves. Having denoted with t_i the time of arrival at a sensor S_i of an AE event generated at point S and at time t_0 , $|S - S_i| = [(x - x_i)^2 + (y - y_i)^2 + (z - z_i)^2]^{1/2}$, the distance between S_i and source S , in Cartesian coordinates, and assuming the material to be homogenous, the path of the signal is given by: $|S - S_i| = v(t_i - t_0)$. If the same event is observed from another sensor S_j at time t_j , it is possible to eliminate t_0 from the equation:

$$|S - S_j| - |S - S_i| = v(t_j - t_i) \equiv v\Delta t_{ji}. \quad (1)$$

Assuming the arrival times of the signals and the positions of the two sensors to be known, Eq. 1 is an

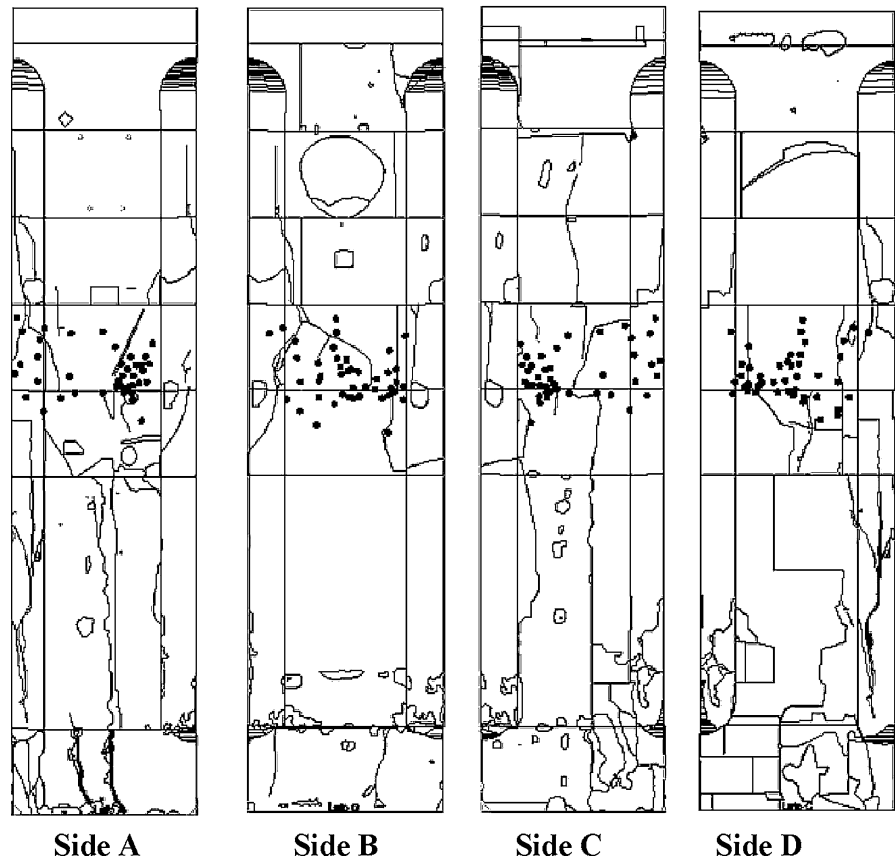
equation with four unknowns, x , y , z and v . Hence, the problem of the localisation of S is determined if it is possible to write a sufficient number of equations such as Eq. 1, i.e., when an AE event is identified by at least five sensors. If this did not occur, it would be necessary to adopt simplifying assumptions to reduce the degrees of freedom of the problem, such as, for instance, imposing the speed of transmission of the signals or having the AE source lie on a plane predetermined.

In the present work, applying the localisation procedure more than 50 AE sources were localised with an high confidence level. Considering previous applications of the AE technique carried out by the authors, the approximation for elements with large size is about $\pm 10 \text{ mm}$ [7]. The localised sources and the cracking pattern for pillar no. 19 are represented in Fig. 9. It can be noted that the localised sources are concentrated near the more visible crack paths. The localisation of these source concentration (Fig. 9) and the oscillation counting (Fig. 8) denounce that the pillar is subject to a damaging phenomenon in slow but progressive evolution.

5.2 Time dependence of damage

We consider that during the microcrack propagation the dissipated energy, E , in a structural element is proportional to the cumulative number of AE counts, N [3, 4, 21]. In this way the time dependence of the structural damage observed during the monitoring period, identified by parameter η , can also be correlated to the rate of propagation of the microcracks. If we express the ratio between the cumulative number of AE counts recorded during

Fig. 9 Cracking pattern and localisation of AE sources for pillar 19



the monitoring process, N , and the number obtained at the end of the observation period, N_d , as a function of time, t , we get the damage versus time dependence on AE:

$$\eta = \frac{E}{E_d} = \frac{N}{N_d} = \left(\frac{t}{t_d}\right)^{\beta_t} \quad (2)$$

In Eq. 2, the values of E_d and N_d do not necessarily correspond to critical conditions ($E_d \leq E_{max}$; $N_d \leq N_{max}$) and the t_d parameter should be construed as the time during which the structure has been monitored. By working out the β_t exponent from the data obtained during the observation period, we can make a prediction as to the structure's stability conditions. If $\beta_t < 1$, the damaging process slows down and the structure evolves towards a stability condition, in as much as energy dissipation tends to decrease; if $\beta_t > 1$, the process diverges and becomes unstable; if $\beta_t \cong 1$ the process is metastable, i.e., though it evolves linearly over time, it can reach indifferently either stability or instability conditions [3, 4, 21].

During the observation period, which lasted 121 days for the monitored pillar, the number of AE counts was $\cong 4300$ (Fig. 8). In order to obtain indications on the rate of the damage process, as given in Eq. 2, the data obtained with the AE technique were subjected to best-fitting in the bilogarithmic plane. This yielded a slant $\beta_t \cong 0.98$ as shown in Fig. 10. The result confirms that the damage process in the pillar is in metastable conditions according to a quasi-linear progression over time.

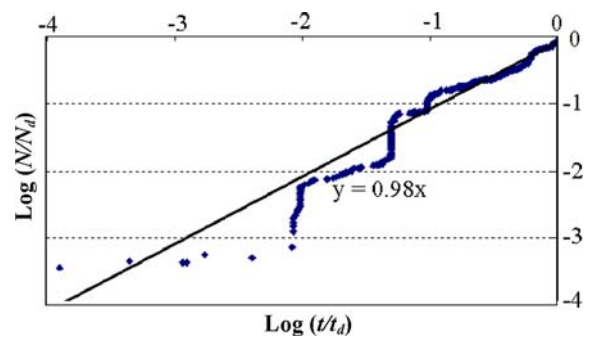


Fig. 10 Evaluation of damage, β_t exponent for pillar 19

6 Numerical simulation

6.1 Laboratory tests and characteristic constants

Beside the experimental research, a numerical simulation based on the Finite Element Method is performed, which is able to catch the main non linear features of the mechanical behaviour such as fracture nucleation, fracture propagation and time dependency. The main goal will be to link the released energy, acquired from the AE, and the fracture localization with the results obtained numerically [9]. To this end a number of tests have been conducted in order to determine the mechanical properties of the Syracuse Cathedral stone.

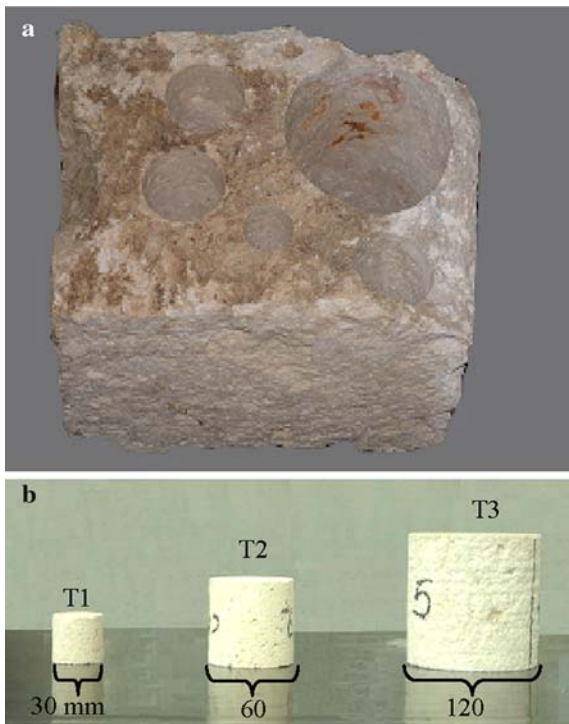


Fig. 11 The stone block (a), and the cylindrical specimens used for the laboratory tests (b)

The ancient stone used in the construction of the temple was located in the area of Plemmirio, just south of Syracuse, where archaeological studies have found the presence of various quarries of the Greek period. During the restoration works recently carried out the technique of replacing stone blocks was employed for several damaged elements. The removed elements were replaced by other blocks consisting of the same stone. In particular, a portion of one of the removed elements has been used to define, through laboratory tests, the mechanical properties of the material that since 2400 years constitutes the bearing structure of the Cathedral (Fig. 11). Some cylindrical specimens having slenderness $\lambda = 1$, and diameter equal to 30, 60 and 120 mm respectively, were obtained from the stone block (Fig. 11a, b). In particular, three specimens with diameter of 30 mm (T1_{a-c}) and 60 mm (T2_{a-c}) were tested, while only two specimens with diameter of 120 mm (T3_{a,b}) were analyzed. The specimens have been subjected to laboratory compressive tests at constant displacement rate of 4×10^{-4} mm/s. Through the laboratory tests the ultimate peak stress (σ_u), and the elastic modulus (E) are computed (see Table 2).

6.2 The numerical model

A detailed 3D model of the most damaged pillar has been obtained according to the geometrical survey. The geometry of each block, as well as the presence of masonry inserts, have been considered. Fifteen-node isoparametric solid wedge elements have been used to discretize the more regular zones of the model, while ten-node, three-side isoparametric solid pyramid elements have been adopted for the more complicated ones. Interfaces between blocks have been modelled with triangular twelve-node quadratic interface elements.

The resulting model comprises 5081 elements and 9188 nodes. Figure 12 shows the mesh of the pillar,

Table 2 Average experimental values obtained from compressive tests

Specimens	Diameter (mm)	Peak load (kN)	Peak stress (σ_u) (MPa)	Elastic modulus (E) (MPa)
T1 (a-c)	30	7.12	10.7	1,500
T2 (a-c)	60	22.10	7.82	2,015
T3 (a,b)	120	96.59	8.54	2,200

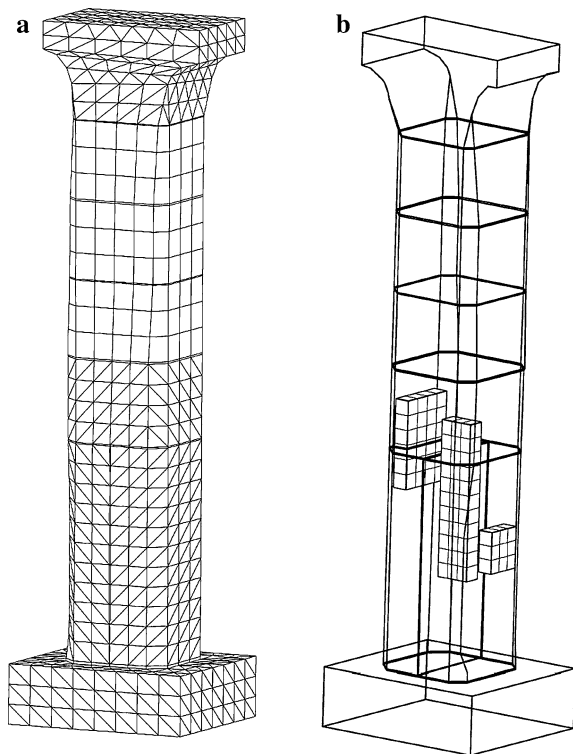


Fig. 12 Finite element mesh of the pillar (a). Details of the masonry inserts (b)

and the details of the masonry inserts acquired by the NDT analysis. The displacements at the base of the pillar were fixed, while the top of the pillar was elastically constrained, in order to account for the interaction with the surrounding structure of the Cathedral. Two main loads were considered: the dead load (of the pillar and of the surrounding structure), and an horizontal seismic load provided as an horizontal ground acceleration.

Figure 13a shows a detail of the interface elements between each block of the pillar, while Fig. 13b shows the deformed mesh under the effect of the dead load. The elastic modulus of the stone block, as deduced from the experimental tests, was 2000 MPa, while the Poisson ratio was equal to 0.12. The mean compressive strength was equal to 9 MPa. For the present sandstone, an average tensile strength of 3 MPa, and a fracture energy of 50 Nm were adopted.

It is worth noting that, under the effect of the sole gravity load, the maximum compressive stress does not exceed the value of 2 MPa, which is low compared to the strength of the sandstone. On the other hand, due to the heterogeneity of the pillar,

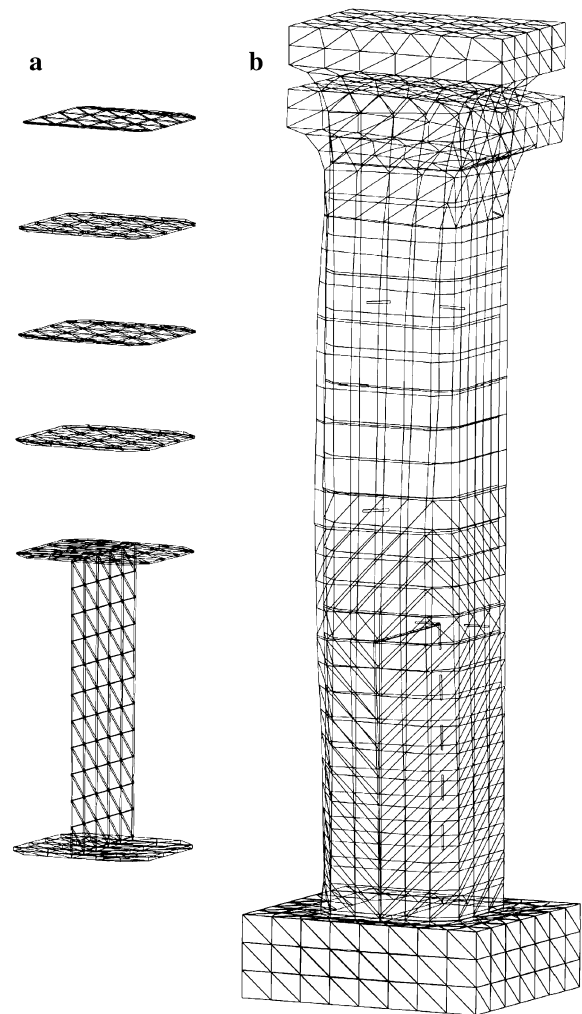


Fig. 13 Detail of the interface finite element mesh between blocks (a). Dead load deformed mesh (b)

tensile stresses may arise that approach the tensile strength.

A seismic load has also been considered. If a return period of 140 years is assumed, an horizontal acceleration of 1.288 m/s^2 is to apply (30% probability occurrence in a period of 50 years). In this case, the compressive and tensile stresses increase, as shown in Fig. 14a. The pillar deforms mainly according to his first modal shape, as shown in Fig. 14b.

Due to the horizontal acceleration, cracking can take place in the pillar. A detail of crack nucleation is shown in Fig. 15. The crack occurrence provided by the analysis agrees quite well with the crack localization provided by the AE recording. Cracking

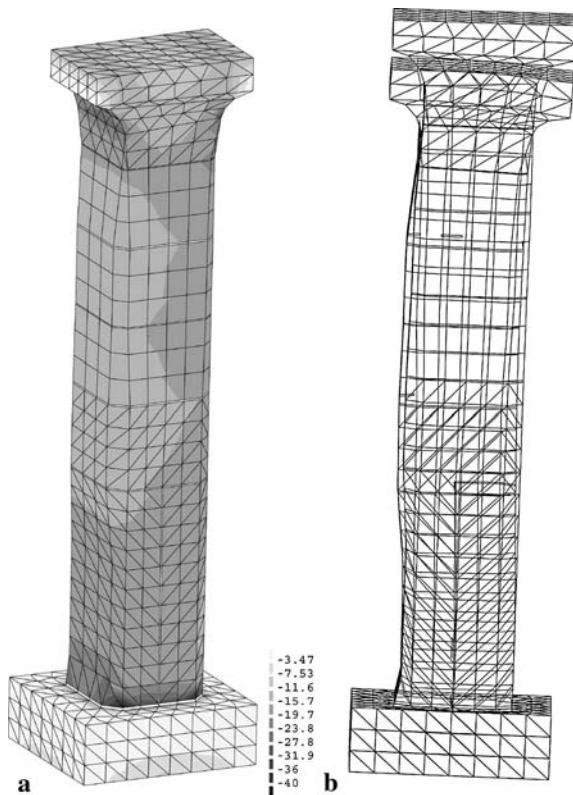


Fig. 14 Principal compressive stress (a). Deformed mesh under the seismic acceleration (b)

corresponds both to diffuse cracking in the continuum elements of the sandstone blocks and to opening or sliding of the discrete interfaces between blocks.

7 Conclusion

The evolution of damage in a pillar made of calcareous stone blocks that is part of the vertical bearing structure of the Syracuse Cathedral was evaluated using the AE technique. The data collected were analysed in order to interpret the evolution of damage and to determine the positions of AE sources within the pillar. From the charts plotted for the differential and cumulative functions of the AE signal counts it can be seen that the pillar is actually undergoing a damage process. Moreover, by applying the AE source localisation procedure it was possible to identify ca. 50 emission points in the pillar. Inside the stone blocks to which the sensors had been applied, the points were seen to concentrate along the

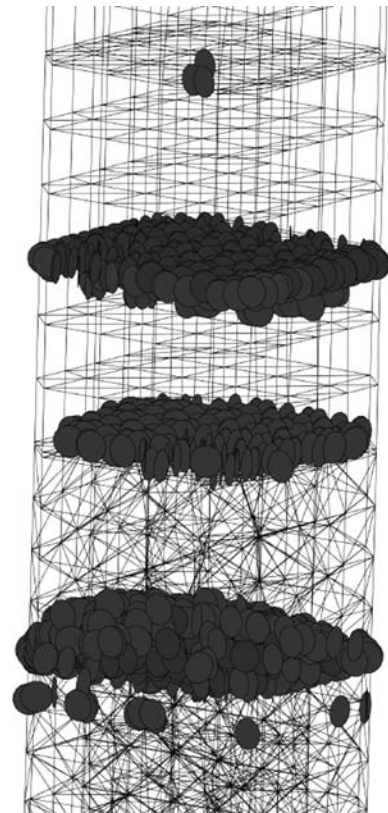


Fig. 15 Cracking in the central zone of the pillar when subjected to the seismic load

cracks that could be discerned more clearly on the surface. The identification of these emission sources together with the counts oscillation shows that the pillar is indubitably undergoing a slow but incessant damage process.

Beside the experimental research, using a numerical simulation based on the Finite Element Method, the most damaged pillar has been modelled in details, providing an accurate description of the blocks interaction by means of discrete interface elements. The numerical analysis has been performed considering the structure subjected to seismic horizontal loads. By this model the crack nucleation is found in the same positions identified through the AE monitoring. In this way the numerical model confirms the results obtained experimentally.

Acknowledgements The financial support provided by the European Union (EU) Leonardo da Vinci Programme, ILTOF Project is gratefully acknowledged. Special thanks for their collaboration go to the Dr. M. Muti, to the Dr. Meloni and to

the Dr. L. Regalbuto from the Syracuse Superintendence for Cultural Heritage.

References

1. Binda L, Casolo S, Petrini V, Saisi A, Sanjust CA, Zanzi L (2007) Evaluation of the seismic vulnerability of the Syracuse Cathedral: investigation and modelling. Proc. of Int. Symposium Studies on Historical Heritage. Yildiz Technical University, Istanbul, Turkey, pp 683–690
2. Carpinteri A, Lacidogna G (2006) Damage monitoring of an historical masonry building by the acoustic emission technique. *Mater Struct* 39:161–167
3. Carpinteri A, Lacidogna G (2006) Structural monitoring and integrity assessment of medieval towers. *J Struct Eng (ASCE)* 132:1681–1690
4. Carpinteri A, Lacidogna G (2007) Damage evaluation of three Masonry Towers by acoustic emission. *Eng Struct* 29:1569–1579
5. Carpinteri A, Lacidogna G, Niccolini G (2006) Critical behavior in concrete structures and damage localization by acoustic emission. *Key Eng Mater* 312:305–310
6. Carpinteri A, Lacidogna G, Paggi M (2006) Acoustic emission monitoring and numerical modelling of FRP delamination in RC beams with non-rectangular cross-section. *Mater Struct (RILEM)* 40:553–566
7. Carpinteri A, Lacidogna G, Manuello A (2007) Damage mechanisms interpreted by acoustic emission signal analysis. *Key Eng Mater* 347:577–582
8. Carpinteri A, Invernizzi S, Lacidogna G (2005) In situ damage assessment and nonlinear modelling of an historical Masonry Tower. *Eng Struct* 27:387–395
9. Carpinteri A, Invernizzi S, Lacidogna G (2008) Cracking simulation of Brick-Masonry subjected to the double Flat-Jack test. In: Proc of structural analysis of historical constructions. Bath, 2–4 July 2008
10. Agnello G (1996) *Il Duomo di Syracuse e i Suoi Restauri*, a cura di S. L. Agnello, Ediprint, Siracusa (in Italian)
11. Agnello SL (1950) *La Rinascita Edilizia a Siracusa Dopo il Terremoto del 1693*, Archivio Storico Siciliano, serie III, vol IV, 1950–1951, Palermo (in Italian)
12. Privitera S (1863) *Illustrazioni sull'Antico Tempio di Minerva Oggi il Duomo di Siracusa*, Memoria del Parroco Serafino Privitera. Tipografia La Fenice Musumeci Catania (in Italian)
13. Russo S (1991) *La Cattedrale di Siracusa*. Archivio Storico Siracusano, III V (in Italian)
14. Russo S (1992) *Siracusa Medievale e Moderna*. Arnaldo Lombardi, Palermo (in Italian)
15. Binda L, Saisi A, Tiraboschi C (2000) Investigation procedures for the diagnosis of historic masonries. *Constr Building Mater ed Elsevier-Norwich* 14(4):199–233
16. Binda L, Lualdi M, Saisi A, Zanzi L (2003) The complementary use of on site non destructive tests for the investigation of historic masonry structures. In: Proc 9th North American Masonry Conference, (9NAMC), pp 978–989
17. Binda L, Cantini L, Condoleo P, Saisi A, Zanzi L (2006) Investigation on the pillars of the Syracuse Cathedral in Sicily. In: Forde MC (ed) *3-Day int conf structural faults & repair*. Engineering Technics Press, Edinburgh, CD-ROM, pp 1–12
18. Brindley BJ, Holt J, Palmer IG (1973) Acoustic emission-3: the use of ring-down counting. *Non-Destr Test* 6: 299–306
19. Pollock AA (1973) Acoustic emission-2: acoustic emission amplitudes. *Non-Destr Test* 6:264–269
20. Swindlehurst W (1973) Acoustic emission-1: introduction. *Non-Destr Test* 6:152–158
21. Carpinteri A, Lacidogna G, Pugno N (2007) Structural damage diagnosis and life-time assessment by acoustic emission monitoring. *Eng Fract Mech* 74:273–289